Received: 14 November 2017 | Revised: 18 June 2018 | Accepted: 13 August 2018

DOI: 10.1002/nag.2856

RESEARCH ARTICLE

WILEY

Global method for stability analysis of anchored slopes

Tan Zhang[1] | Hong Zheng[2] | Cong Sun[2]

[1]Key Laboratory of Urban Security and Disaster Engineering (Beijing University of Technology), Ministry of Education, Beijing 100124, China

[2]State Key Laboratory of Geomechanics and Geotechnical Engineering, Institute of Rock and Soil Mechanics, Chinese Academy of Sciences, Wuhan 430071, China

Correspondence
Hong Zheng, State Key Laboratory of Geomechanics and Geotechnical Engineering, Institute of Rock and Soil Mechanics, Chinese Academy of Sciences, Wuhan 430071, China.
Email: hzheng@whrsm.ac.cn

Funding information
National Natural Science Foundation of China, Grant/Award Numbers: 51538001 and 11172313; National Basic Research Program of China, Grant/Award Number: 2014CB047100

Summary

Based on the global method, an approach is proposed to consider the effect of anchor reinforcement on slope stability, where equilibrium conditions are formulated in terms of the whole slip body. Anchor pre-tension is assumed to be undertaken by the whole slip body instead of individual slices, causing internal force within slope more realistic. Meanwhile, the optimization model for locating the critical slip surface is of weak nonlinearity and easy to solve using the conventional optimization procedures. The effects of anchoring orientation and position are thoroughly investigated, and interesting results are obtained.

KEYWORDS

anchors, global method, limit equilibrium method, slopes, stabilization

1 | INTRODUCTION

In the recent decades, to prevent and control landslide disasters, pre-tensioned anchors are increasingly used to stabilize dangerous slopes, especially slopes in highway and hydraulic power engineering. Anchors have significant technical advantages, such as saving substantial cost and reducing construction period. Nevertheless, the stability analysis of anchored slopes has been little touched upon in the classic literature, even in those monographs dealing with various aspects of slope stability analysis and stabilization methods, such as Abramson et al[1] and Bromhead.[2]

A few of methods, however, were developed to carry out the stability analysis of anchored slopes. Cai and Ugai[3] studied the reinforcing mechanism of anchors in slopes using the finite element method and the Bishop method of slices, where the safety factors of anchored slopes were calculated and compared with each other. Although the finite element method, which satisfies both equilibrium and compatibility requirements, has indeed advantages over the limit equilibrium methods in many aspects,[4] the limit equilibrium methods have final say in the codes of slope engineering. The reason for this is due in part to the fact that using a few of geotechnical parameters, the information on the slope stability can be obtained directly with the limit equilibrium methods, and the results can still meet the accuracy requirements in the actual construction.

In practical applications, the stability analysis of anchored slopes is normally carried out by extending the existing methods, such as the methods of slices and finite element method, to incorporate forces exerted by anchors. For example, Hryciw[5] considered the action of anchors as discrete surface loads and used in the infinite slope theoretical analysis to determine the optimum orientation of anchors in cohesionless soils. To analyze the reliability of anchored slopes considering stochastic corrosion of anchors, a methodology using the Monte Carlo simulation was developed in conjunction

with the method of slices in Li et al.[6] The normal stress on the slip surface purely induced by the anchor load was taken as the analytical elastic stress distribution in an infinite wedge approximating the slope geometry; Zhu et al[7] analyzed anchored slopes by a distribution of tractions acting on the slice bottoms and statically equivalent to the point forces of the anchors. Since the distribution of tractions is from the wedge solution from elasticity, it is beyond the assumption that the sliding body is actually a rigid body in the context of limit equilibrium methods. Li et al[8] proposed a procedure based on the kinematic limit analysis to consider the reinforcing effect of anchors on slope stabilization.

Since Bishop,[9] all rigorous methods of slices chose to eliminate the normal pressure on the slice bottom from the equilibrium equations and place the burden of static indeterminacy on the interslice forces. Bell[10] first proposed another way to overcome the difficulties encountered in the rigorous methods of slices through introducing a distribution of normal pressure along the slip surface. The same idea was utilized in Zhu and Lee,[11] with a different assumption on the distribution of normal pressure from Bell.[10] Later on, Zheng et al[12] proposed the realistic distribution, form which the normal pressure on the slip surface follows, and proposed a simple scheme for approximating the normal pressure along the slip surface. Since the whole slip body instead of individual slices, this method is named the global method in Zheng and Zhou.[13] The solution to the factor of safety in the global method turns out to be an algebraic eigenvalue problem,[14] and accordingly it has no issue in convergence, because an eigenvalue problem always has a solution, which can be found within a finite number of algebraic operations.

Compared with the solution of the factor of safety for a given slip surface, the location of the critical slip surface, on which the factor of safety attains its minimum, is far more difficult in that it actually reduces to an optimization problem. The optimization models induced by the conventional methods of slices have so strong nonlinearity that usually one has to resort to those sophisticated optimization techniques. Cheng et al did deep and thorough researches on the search for critical slip surfaces.[15,16]

Together with the Spencer method, Baker proposed a dynamic programming for determining the critical slip surface,[17] which was extended in Yamagami and Jiang,[18] to search for the three-dimensional critical slip surfaces, together with the simplified Janbu method. Chen and Shao[19] employed the simplex method, steepest descent, and the Davidson-Fletcher-Powell method in conjunction with a grid search solution, and had an important finding that the factor of safety might have multiple minima. In order to avoid being trapped in local minima, Li et al[20] adopted a real-coded genetic algorithm, and Cheng et al[21] applied artificial fish swarms algorithm.

On the basis of the sliding field conception along with the Spencer method, Zhu et al presented a method for locating critical slip surfaces of general shapes in slope stability analysis,[22] which involves a number of trial and error operations.

In addition to the solution of the factor of safety associated with a given slip surface, this study also sets up a global method-based optimization model for locating the critical slip surface of an anchored slope. Different from any other optimization procedures in the literature, the proposed optimization model has a linear objective function with the constraints being at most cubic polynomials and, consequently, can be easily solved using those conventional optimization techniques, with no need to resort to those sophisticated optimization techniques.

2 | GLOBAL METHOD OF STABILITY ANALYSIS OF ANCHORED SLOPES

Shown in Figure 1 is a schematic of a sliding body Ω reinforced using two rows of pre-tensioned anchors with the borehole points at K_1 and K_2. The sliding body is supposed to be represented by a planar region Ω that is encompassed by the

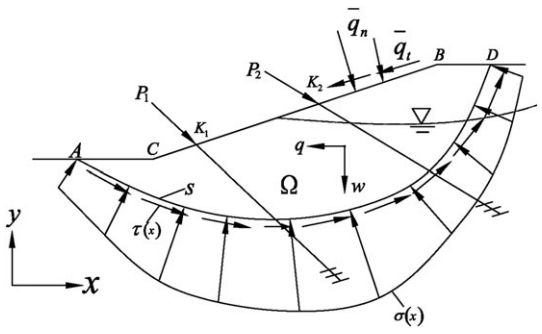

FIGURE 1 System of forces on an anchored slope

ground surface *DBCA*, the slip surface represented by the curve *AD* will be designated subsequently by *S*. Ω may contain multiple subregions each of which represents a type of soil.

The external forces acting on Ω might include the body forces: the vertical gravity w and the horizontal seismic force q; the surface loads: the normal traction $\overline{q}_n$ and the tangential traction $\overline{q}_t$ along the ground surface *DBCA;* and the pre-tension P_j of the j-th row of anchors fixed at the borehole point $K_j\left(x_j^p, y_j^p\right)$ on the ground surface.

Acting along the slip surface S are the constraint forces of the total normal stress $\sigma(x)$ and shear stress $\tau(x)$.

Temporally, let the slip surface S be given. In formulating the equilibrium conditions, the whole slip body Ω is take as the loaded object. Taking three arbitrary points $\left(\overline{x}_i^c, \overline{y}_i^c\right)$, i =1, 2, 3, which are not on the same straight line, as the moment centers, respectively, the resultant moments of forces acting on Ω about $\left(\overline{x}_i^c, \overline{y}_i^c\right)$ should vanish, that is

$$\int_S \left(\Delta x_i^c \sigma - \Delta y_i^c \tau\right) dx + \left(\Delta x_i^c \tau + \Delta y_i^c \sigma\right) dy + m_i^c = 0 \tag{1}$$

where Δx_i^c and Δy_i^c are the components of the vector from $\left(\overline{x}_i^c, \overline{y}_i^c\right)$ to point (x, y) on the slip surface S, namely,

$$\Delta x_i^c = x - \overline{x}_i^c, \quad \Delta y_i^c = y - \overline{y}_i^c. \tag{2}$$

The index i represents a free index. In other words, whenever the index i appears in an equation, i will traverse 1, 2, and 3, and three relevant equations similar in form will be derived by taking in turn the three points $\left(\overline{x}_i^c, \overline{y}_i^c\right)$, i =1, 2, 3, as the moment center. For simplicity in presentation, the slope is assumed to ascend as a whole along the positive x-axis.

m_i^c in Equation 1 represents the resultant moment of all the external forces acting in/on Ω about $\left(\overline{x}_i^c, \overline{y}_i^c\right)$, amongst which is gravity, which can be calculated with the boundary integrals, and accordingly the partition of slices is no longer needed, with more details in Zheng and Tham.[12]

Due to the complicated soil-anchor interaction and other uncertainties, in the methods of slices, the action of pre-tensioned anchors is usually simplified as the point force acting on only one slice at which the anchor borehole is. This, however, may lead to an abrupt change in the normal stress distribution along the slip surface.[5] To account properly for the effect of anchors on the whole slope, let P_j denote pre-tension in the jth row of anchors acting at the borehole point $K_j\left(x_j^p, y_j^p\right)$ on the ground surface at an angle of β_j with the negative x-axis, as shown in Figure 1. All the n^p rows of pre-tensioned anchors do contribution to the total moment m_i^c about $\left(\overline{x}_i^c, \overline{y}_i^c\right)$, represented by m_i^p, reading

$$m_i^p = -\sum_{j=1}^{n^p} P_j \left[\left(x_j^p - \overline{x}_i^c\right) \sin\beta_j + \left(y_j^p - \overline{y}_i^c\right) \cos\beta_j\right]. \tag{3}$$

Once m_i^p is calculated, it is added to the total moment m_i^c in Equation 1.

The treatment of anchors in the above is simpler than that in Zhu et al,[7] where the action of point forces in the anchors leads to a distribution of tractions acting on the slip surface and determined by the wedge solution from elasticity, which is accurate only for homogeneous materials. In this study, the anchoring forces, P_j, are undertaken by the whole slip body, which is deemed rigid in the context of limit equilibrium methods.

Suppose that the Mohr-Coulomb criterion holds along the slip surface S. When the anchored slope is in the state of limit equilibrium, along S we have

$$\tau = \frac{1}{F}[c_e + f_e(\sigma - u)] = \frac{1}{F}(c_w + f_e \sigma) \tag{4}$$

where F is the factor of safety, c_e and f_e are effective shear strength parameters, u is pore pressure, and $c_w = c_e - f_e u$.

Substituting Equation 4 into Equation 1, it is followed that

$$\int_S L_i^x \sigma dx + L_i^y \sigma dy + m_i^c F + d_i^c = 0 \tag{5}$$

where

$$L_i^x = F\Delta x_i^c - f_e \Delta y_i^c, \quad L_i^y = F\Delta y_i^c + f_e \Delta x_i^c \tag{6}$$

$$d_i^c = \int_S c_w \Delta x_i^c dy - c_w \Delta y_i^c dx. \tag{7}$$

The real distribution of total normal stress along the slip surface should take the form.[12]

$$\sigma = \sigma(x) = \sigma_0 + \sigma_I \tag{8}$$

where σ_0 is caused merely by the body forces, which is also a major part of σ; σ_I is reflecting the action of the sliding body on other external forces excluding the body forces. Both σ_I and σ_0 are the function of x.

For simplicity, we only consider the situation where only gravity and no seismic load is present. In this case,

$$\sigma_0 = \sigma_h \cos^2\alpha \tag{9}$$

where

$$\sigma_h = \int_{y_H}^{y_G} \gamma dy. \tag{10}$$

y_H and y_G are the y-coordinates of the two points $H(x_H, y_H)$ on the slip surface S and $G(x_H, y_G)$ on the ground surface, which are the intersection points of the vertical line $x = x_H$ with the slip surface S and the ground surface, respectively; α is the angle of the slip surface S at the point H with axis-x, and γ is the natural unit weight along the vertical line HG.

σ_I in Equation 8 is indeterminate. To make the problem statically determinant, at most two unknowns can be introduced, namely,

$$\sigma_I = f(x; a, b) \tag{11}$$

where a and b are two parameters to be solved. Zheng and Tham[12] proposed a linear function $f(x; a, b)$ be used to approximate σ_I, namely

$$f(x; a, b) = a l_a(x) + b l_b(x) \tag{12}$$

with

$$l_a(x) = -\frac{x - \overline{x}_b}{\overline{x}_b - \overline{x}_a}, \quad l_b(x) = \frac{x - \overline{x}_a}{\overline{x}_b - \overline{x}_a} \tag{13}$$

$\overline{x}_a$ and $\overline{x}_b$ being x-coordinates of any two points not in a vertical line, for example, the slope toe and top, respectively.

Substituting Equation 12 into system (4), the system of three equations in F, a, and b follows

$$\mathbf{g}(F, a, b) \equiv F(a\mathbf{u}_1 + b\mathbf{u}_2 + \mathbf{u}_3) + a\mathbf{u}_4 + b\mathbf{u}_5 + \mathbf{u}_6 = 0 \tag{14}$$

where $\mathbf{g}$ is a three-dimensional vector-valued function in F, a, and b; $\mathbf{u}_1$ to $\mathbf{u}_6$ are three-dimensional vectors, defined as

$$u_{1,i} = \int_S \Delta x_i^c l_a dx + \Delta y_i^c l_a dy \tag{15}$$

$$u_{2,i} = \int_S \Delta x_i^c l_b dx + \Delta y_i^c l_b dy \tag{16}$$

$$u_{3,i} = m_{ci} + \int_S \Delta x_i^c \sigma_0 dx + \Delta y_i^c \sigma_0 dy \tag{17}$$

$$u_{4,i} = -\int_S f_e \Delta y_i^c l_a dx - f_e \Delta x_i^c l_a dy \tag{18}$$

$$u_{5,i} = -\int_S f_e \Delta y_i^c l_b dx - f_e \Delta x_i^c l_b dy \tag{19}$$

$$u_{6,i} = -\int_S (c_w + f_e \sigma_0) \Delta y_{ci} dx - (c_w + f_e \sigma_0) \Delta x_{ci} dy. \tag{20}$$

Solving for a and b from the first two equations in system (14) and then substituting them into the third equation, a cubic polynomial equation in F is derived. Since a cubic polynomial equation has at least one real root, system (14) has at least one real solution, and again no convergence issue exists for the global method.

We notice here that the failure of anchors must be taken into account in the design of slope reinforcements. Usually, failure of anchors is caused by slope deformation if no chemical action is ignored. In such cases, more complicated analysis, such as the finite element analysis, must be carried out.

3 | DETERMINATION OF THRUST LINE OF REINFORCED SLOPES

Once the solution to system (14) is obtained, we can calculate the interslice forces to check whether the solution leads to a statically admissible system of forces on the slip body.

Suppose that a vertical line MN at $x = x_o$ divides the sliding body Ω into two parts, as show in Figure 2, and take the lower part Ω_L as the loaded body.

Considering the two conditions of force equilibrium in the horizontal and vertical directions, respectively, we can obtain the interslice forces t_h and t_v

$$t_h = -q_L + \int_L q_t dx - q_n dy + \sum_{j=1}^{n^p} P_j \cos\beta_j \tag{20}$$

$$t_v = -w_L + \int_L q_n dx + q_t dy - \sum_{j=1}^{n^p} P_j \sin\beta_j \tag{21}$$

where L represents the anticlockwise outer boundary of Ω_L excluding MN; q_n and q_t are normal and tangential tractions along L:$q_n = \overline{q}_n$,$q_t = \overline{q}_t$ on the ground surface NCA, and q_n=σ,q_t=τ on the slip surface AM; w_L is the gravity of Ω_L and q_L is the seismic load. If the anchor borehole point $\left(x_j^p, y_j^p\right)$ is outside Ω_L, let $P_j = 0$.

Take the origin (0, 0) as the moment center and use the condition of moment equilibrium to compute the ordinate y_0 of the action point T of the interslice force (t_h,t_v), we have

$$y_0 = \frac{1}{t_h}\left[x_0 t_v - m_L - \int_L (xq_n - yq_t)dx + (xq_t + yq_n)dy + \sum_{j=1}^{n^p} P_j\left(x_j^p \sin\beta_j + y_j^p \cos\beta_j\right)\right] \tag{22}$$

where m_L is the moment of w_L and q_L around the origin.

4 | LOCATION OF CRITICAL SLIP SURFACE OF ANCHORED SLOPES

On the basis of the global method of slope stability analysis, Sun et al[23] proposed an optimization model for locating the critical slip surface with no anchor reinforcement. Here, we extend this model to the analysis of anchored slopes.

First, a series of vertical lines with x-coordinates x_k, $k = 1, \cdots, n$, are deployed in a scope in which the critical slip surface might be. Then, let any slip surface in consideration be approximated by connecting points (x_k,y_k) successively on these vertical lines, where the y_k coordinates are the optimization variables.

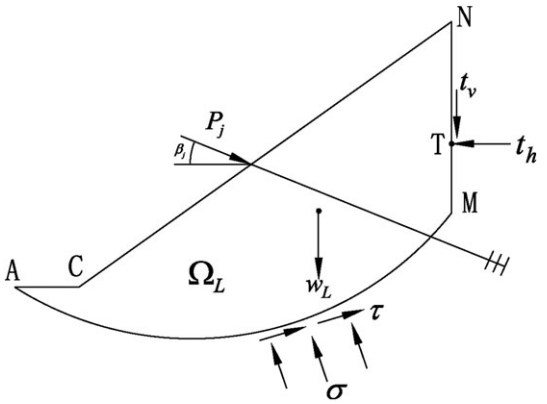

FIGURE 2 System of forces on an anchored slope

Here, in order to simplify programming, let the slip surface pass through all the vertical lines by regarding some ground surface lines as the portions of the whole slip surface. Take Figure 3 as an example, where 50 vertical lines are deployed. Let the slip surface start at the 5th point near the toe, and end at the 46th point on the top. Yet, the lines passing through points (x_1, y_1) to (x_5, y_5) and points (x_{46}, y_{46}) to (x_{50}, y_{50}), which are all on the ground surface, are still regarded as the portions of the slip surface, denoting by S_V these portions on the slope surface, with the subscript "V" representing "Virtual." In the search for the critical slip surface, let the integrals on S_V in Equations 15 to 20 vanish, which is equivalent to letting the normal stress σ on S_V vanish. In this way, the dimensionality of optimization vectors keeps invariant, greatly simplifying the programming.

In the literature the safety factor acts as the objective function, which is an implicit function of y_k, $k = 1, \cdots, n$, denoted by $G(\mathbf{y})$, with the n-dimensional vector $\mathbf{y}$ listing all the y_k.

$G(\mathbf{y})$ induced by a method of slices is usually high nonlinear, leading to huge difficulties in minimizing $G(\mathbf{y})$ subject to the constraints that take on strong nonlinearity as well.

In this study, in order to reduce nonlinearity in the optimization model to be built, the safety factor F will act as an ordinary optimization variable, in the same status as other variables, namely, a and b in Equation 14, and y_k. That is to say, let the objective function $G(F, a, b, \mathbf{y})$ take on the form

$$G(F, a, b, \mathbf{y}) = F. \tag{23}$$

In this way, the objective function becomes an explicit function of the optimization variables.

In addition to three moment equilibrium equations, convexity of the slip surface should act as a constraint, stating that any three adjacent points (x_{j-1}, y_{j-1}), (x_j, y_j), and (x_{j+1}, y_{j+1}) on the slip surface should take on the anticlockwise direction,

$$\det \begin{vmatrix} 1 & x_{j-1} & y_{j-1} \\ 1 & x_j & y_j \\ 1 & x_{j+1} & y_{j+1} \end{vmatrix} \geq 0 \tag{24}$$

if (x_j, y_j) is inside the slip body.

To this point, the optimization model for locating the critical slip surface can be stated as follows. Minimize $G(F, a, b, \mathbf{y})$ subject to system (14) and inequalities (24).

In fact, the constraints of system (14) and inequalities (24) dictate a polyhedral domain in the $(n + 3)$-dimensional space, represented by D, in which the dimensionality n is for vector $\mathbf{y}$ and 3 for the parameters F, a, and b. The above optimization problem is actually to find out the vertex of the polyhedron D with the greatest F-coordinate.

Since the objective function $G(F, a, b, \mathbf{y})$ is linear, and the constraint functions in system (14) are at most cubic polynomials of the optimization variables F, a, b, and y_k if the slip surface is approximated by the line segments (x_1, y_1)- (x_2, y_2), $\cdots$, (x_{n-1}, y_{n-1})-(x_n, y_n), the model has weak nonlinearity and can be solved easily using those commercial software products, such as the function "fmincon" in the Matlab toolbox.

5 | ILLUSTRATIVE EXAMPLES

In this section, the anchor parameters are kept invariant, including the anchor pre-tension P, the anchor borehole position parameter l_x that is the horizontal distance of the borehole point K to the slope toe C, and the anchor inclination β. The effect of these parameters on the stability will be expounded in the next section.

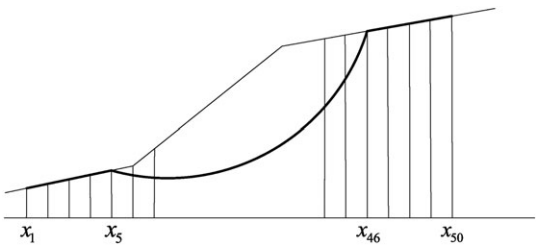

FIGURE 3 All thick lines are regarded as portions of a slip surface

All the examples are analyzed using the global method and the Spencer method implemented in "Slide," a commercial software product by Canadian company Rocsciences.

Example 1. An homogeneous slope

Figure 4 displays a cross section of a homogeneous earth slope with a height of 20 m and a gradient of 2:1. A row of anchors are installed with the anchor parameters as follows: pre-tension P= 600 KN/m-z, the borehole position parameter l_x= 20 m, or the borehole point K(40, 30), and the anchor inclination $\beta = 20°$. Hereafter, "/m-z" in the unit of pre-tension P means "per meter in z-direction."

Figures 5 and 6 display the critical slip surface without and with anchor reinforcement, together with the safety factors in the parentheses. Apparently, with anchor reinforcement, the safety factor does become bigger, yet the critical slip surface gets deeper.

Example 2. A nonhomogeneous slope

Shown in Figure 7 is a section of the nonhomogeneous slope in study, with the anchor borehole point K(40, 30), equivalent to l_x=20 m, anchor inclination $\beta = 20°$ and pre-tension P=150 KN/m-z.

Figures 8 and 9 have the same remarks as Figures 5 and 6.

From the above analyses, the safety factors assessed by the global method are a little bit smaller than those by the Spencer method, by less than 5%. From the practical point of view, such a difference is rather small. Meanwhile, the critical slip surfaces assessed by the two methods agrees well. As we pointed out in the above, however, the global method is completely free from the convergence issue.

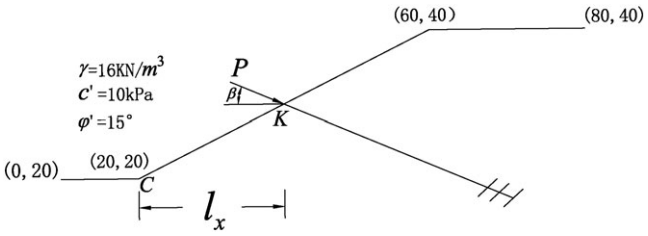

FIGURE 4 Illustrative example 1 of a slope reinforced with anchors

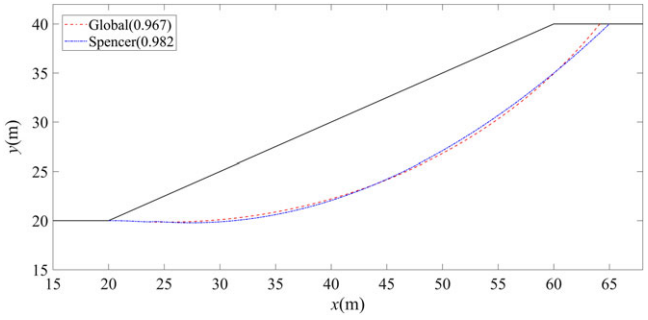

FIGURE 5 Critical slip surfaces of example 1 without anchor reinforcement [Colour figure can be viewed at wileyonlinelibrary.com]

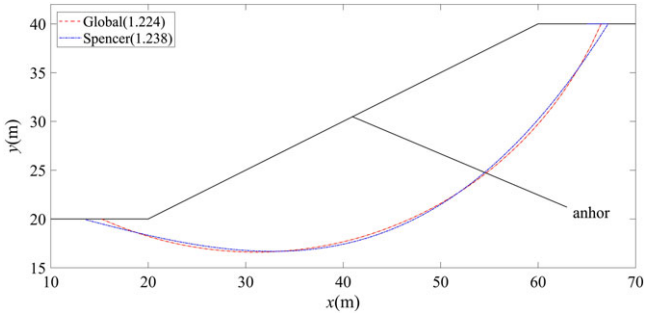

FIGURE 6 Critical slip surfaces of example 1 with anchors (l_x = 20 m, $\beta = 20°$) [Colour figure can be viewed at wileyonlinelibrary.com]

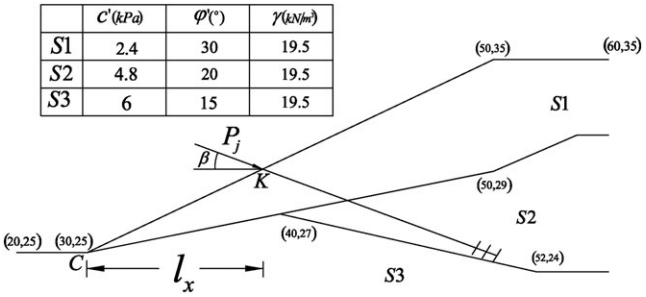

FIGURE 7 A nonhomogeneous slope reinforced with anchors

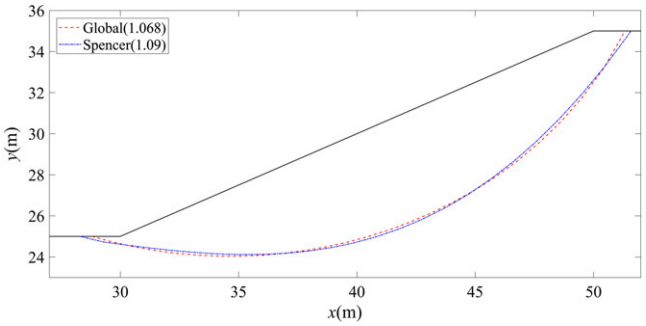

FIGURE 8 Critical slip surfaces of example 2 without anchors [Colour figure can be viewed at wileyonlinelibrary.com]

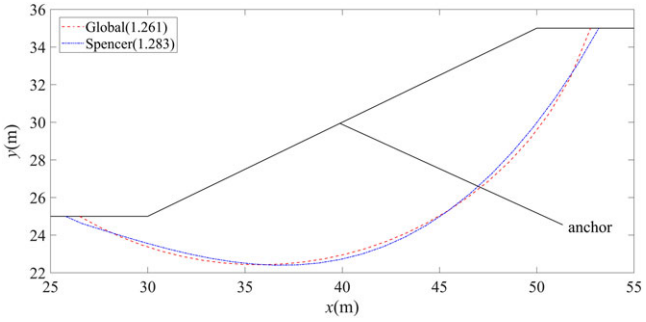

FIGURE 9 Critical slip surfaces of example 2 with anchors ($l_x = 20$ m, $\beta = 20°$) [Colour figure can be viewed at wileyonlinelibrary.com]

6 | FURTHER COMPARISON AND DISCUSSION

In this section, we make a deeper comparison between the global method and the Spencer method, including the normal stress on the slip surface and the thrust line. For cohesionless soil slopes, Hryciw[5] carried out the similar investigation and drew the similar conclusions.

The normal stress distribution along the slip surface of the two examples with the anchor reinforcement is shown in Figures 10 and 11.

From Figures 10 and 11, the curve of the normal stress distribution along the slip surface assessed by the global method is smooth, while by the Spencer method, an abrupt change is observed at the same x-coordinate as the borehole point *K*. We believe that the result by the global method is more reasonable, in that the curve assessed by the Spencer method is strongly dependent on the slice partition. This is further verified in Figures 12 and 13, which display the curve of normal stress distribution along the slip surface with different slice partition.

The abnormal result can be explained as follows. The anchor pre-tension is loaded on only one slice in the Spencer method, and the pre-tension is balanced merely by the normal stress on the bottom of this slice. Due to the static equivalence of the thrust in the slip body, the area under the curve of normal stress distribution along the slip surface is kept invariant with different slice partition. As a result, the greater the number of slices is used in the Spencer method, the more abrupt change will be.

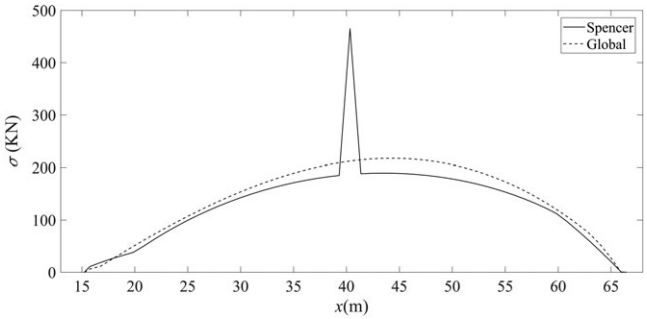

FIGURE 10 Normal stress on slip surface of example 1 with anchors ($l_x = 20$ m, $\beta = 20°$)

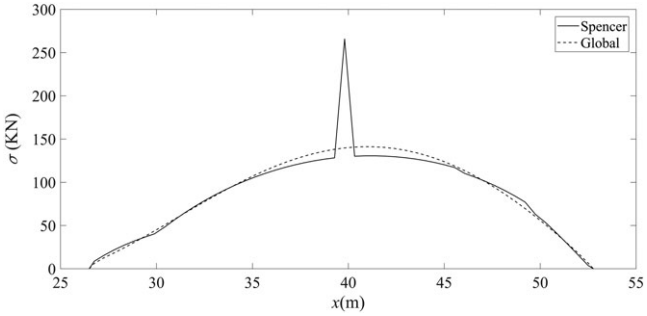

FIGURE 11 Normal stresses on slip surface of example 2 with anchors ($l_x = 20$ m, $\beta = 20°$)

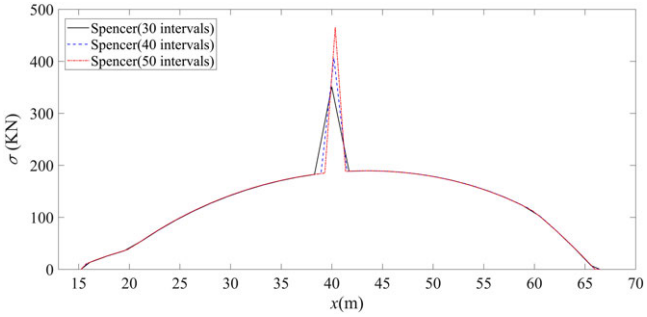

FIGURE 12 Normal stresses on slip surface of example 1 with distinct slice partition ($l_x = 20$ m, $\beta = 20°$) [Colour figure can be viewed at wileyonlinelibrary.com]

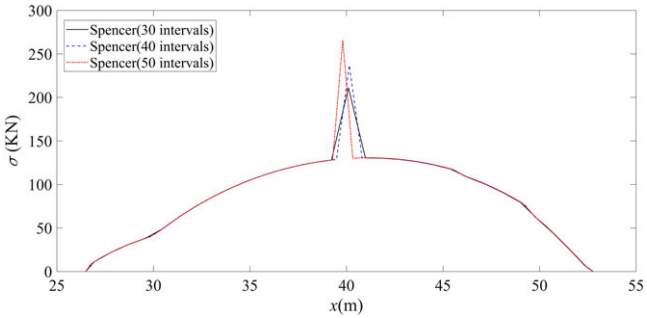

FIGURE 13 Normal stress on slip surface of example 2 with distinct slice partition ($l_x = 20$ m, $\beta = 20°$) [Colour figure can be viewed at wileyonlinelibrary.com]

While in the global method, the anchor pre-tension is undertaken by the whole slip body and, accordingly, no stress concentration is present on the slip surface.

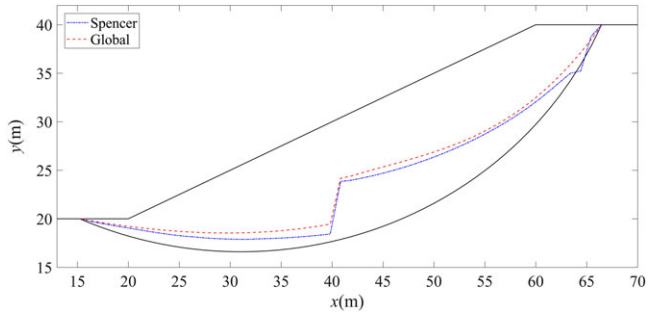

FIGURE 14 Thrust lines of anchored slope with of example 1 ($l_x = 20$ m, $\beta = 20°$) [Colour figure can be viewed at wileyonlinelibrary.com]

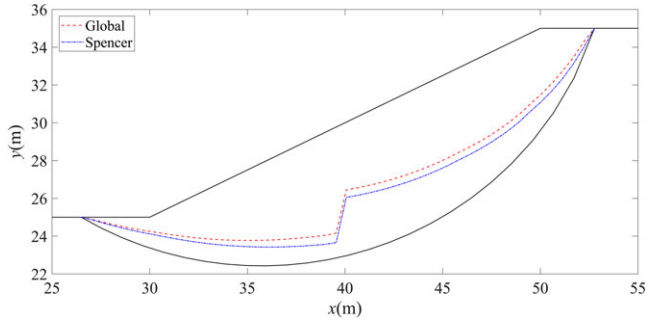

FIGURE 15 Thrust lines of anchored slope with of example 2 ($l_x = 20$ m, $\beta = 20°$) [Colour figure can be viewed at wileyonlinelibrary.com]

Figures 14 and 15 suggest that the thrust lines in the slip body evaluated by the global method and the Spencer method agree well with each other, and both have abrupt changes near the anchor borehole.

7 | EFFECT OF ANCHORING PARAMETERS ON STABILITY

In this section, let the orientation and position of anchors change to look at the effect of these parameters on the slope stability.

7.1 | Effect of anchor orientation

Figure 16 shows the influence of the anchor orientation on the safety factor of example 1, with pre-tension $P = 600$ KN/m-z and the anchor borehole point $K(40, 30)$ keeping invariant, but the anchor inclination β varying from 0° to 45°. As β increases from 0° to 45°, the safety factor decreases from 1.228 to 1.144.

Figure 17 shows the influence of the anchor orientation on the safety factor of example 2, with $P = 150$ KN/m and $K(40, 30)$ keeping invariant, and β varying from 0° to 45°. As β increases from 0° to 45°, the safety factor decreases from 1.272 to 1.131.

The difference of the safety factor calculated by the global method and the Spencer method is always less than 5%. Both the methods have the same trend as the anchor angle β changes. The result is explained as follows. The larger the angle β is, the larger the friction on the slip surface purely caused by the anchor pre-tension is, but the smaller the

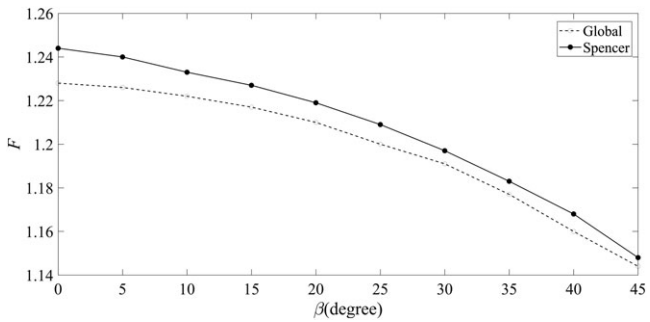

FIGURE 16 Anchor angle β versus safety factor of example 1 ($l_x = 20$ m and $P = 600$ KN/m-z)

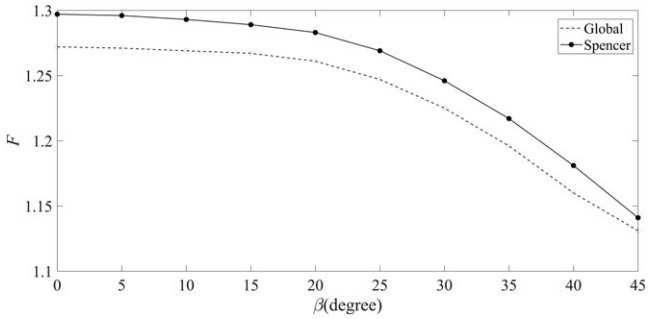

FIGURE 17 Anchor angle β versus safety factor of example 2 (l_x = 20 m and P = 150 KN/m-z)

hauling force of the anchor against slope sliding is. The above results indicate that the stabilization effect of anchors is due mainly to the pre-tension that directly hauls the slip body against sliding down.

7.2 | Effect of anchor position

Apparently, the anchoring position is of interest to the stability of the anchored slope, determining the critical slip surface and the associated safety factor.

Figure 18 illustrates the influence of anchoring position on the safety factor of the slope in example 1 with P = 600 KN/m-z and $\beta = 20°$ keeping invariant. Let the anchoring position parameter l_x vary from 0 to 50 m. It can be seen that the maximum safety factor is attained at l_x= 20 m, with the critical slip surface shown in Figure 6.

Figure 19 shows the influence of anchoring position on the safety factor of the slope in example 2 with P = 150 KN/m-z and $\beta = 20°$ invariant. Let l_x vary from 0 to 22 m. The same variation of the safety factor is observed as in example 1, but the maximum safety factor is attained at l_x= 4 m, with the critical slip surface shown in Figure 20. Noticeably, a very interesting result is observed—*the anchor is outside the critical slip body*! The result appears strange to us at the first glance, yet it is explainable and greatly significant. The critical slip surface of a slope always exists, and the installation of the anchor at some place forces the critical slip surface therein to move to other place but enhances the global stability of the whole slope.

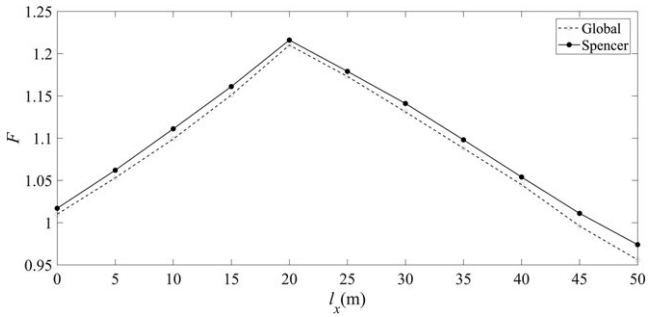

FIGURE 18 Anchoring position l_x versus safety factor of example 1 ($\beta = 20°$ and P = 600 KN/m-z)

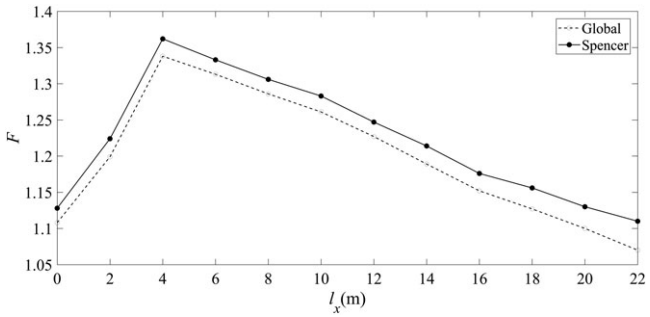

FIGURE 19 Anchoring position l_x versus safety factor of example 2 ($\beta = 20°$ and P = 150 KN/m-z)

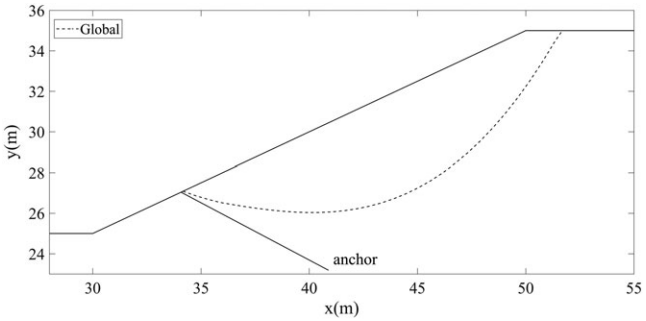

FIGURE 20 Critical slip surface corresponding to best l_x (4 m) at which the maximum safety factor attains (example 2, $\beta = 20°$ and $P = 150$ KN/m-z)

The anchoring position determines the critical slip surface and the associated safety factor.

As another two extreme cases from example 1, if the anchor borehole is very close to the slope toe or the slope top, the anchor will be outside the critical slip body. Figures 21 and 22 display the two extremities.

7.3 | Application of two rows of anchors

If the pre-tension force to reach the given stability cannot be undertaken by one row of anchors, more rows of anchors are needed. Here is such a case.

For the slope of Example 2, the pre-tension of 150 KN/m-z is assumed to be undertaken by two rows of anchors, with the first row of anchors having the anchoring parameters, see Figure 7, $l_x^1 = 20$ m and pre-tension P_1=100 KN/m-z, and the second row of anchors having the anchoring parameters $l_x^2 = 25$ m and pre-tension P_2=50 KN/m-z. All the anchors have the same fixing angle of 20°.

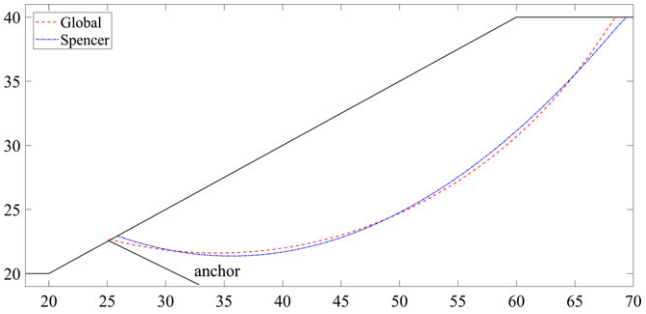

FIGURE 21 Critical slip surface in example 1 with anchors close to slope toe ($l_x = 5$ m, $\beta = 20°$) [Colour figure can be viewed at wileyonlinelibrary.com]

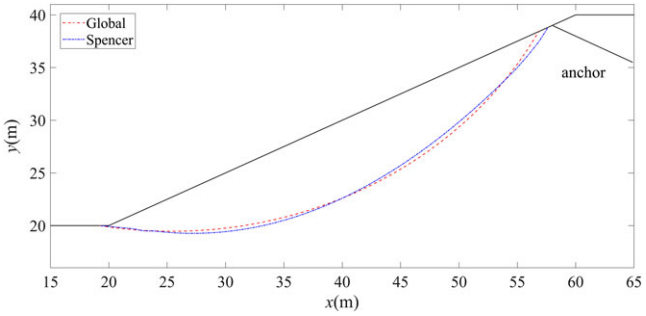

FIGURE 22 Critical slip surface in example 1 with anchors close to slope top ($l_x = 38$ m, $\beta = 20°$) [Colour figure can be viewed at wileyonlinelibrary.com]

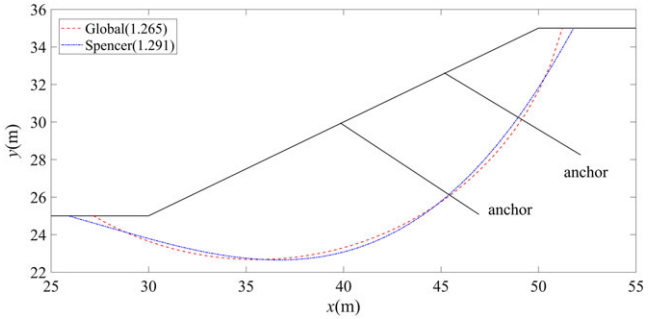

FIGURE 23 Results of example 2 with two rows of anchors ($l_x^1 = 20\text{m}$, $\beta = 20°$; $l_x^2 = 25\text{m}$, $\beta = 20°$) [Colour figure can be viewed at wileyonlinelibrary.com]

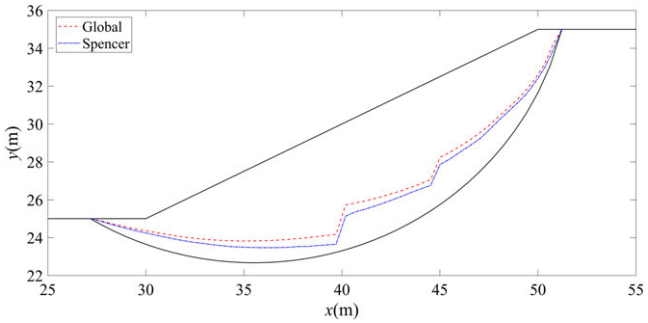

FIGURE 24 Thrust lines of slope in example 2 resulting from two rows of anchors [Colour figure can be viewed at wileyonlinelibrary.com]

Let us return to Figure 9, which displays the results corresponding to one row of anchors applying a pre-tension of 150 KN/m-z, $F_{Global} = 1.261$ and $F_{Spencer} = 1.283$. After applying two rows of anchors, see Figure 23, the results are $F_{Global} = 1.265$ and $F_{Spencer} = 1.291$.

The application of two rows of anchors does not lead to a significant increase in the factor of safety, which is explainable because the improvement of slope stability is due mainly to the reinforcement force (Figure 24).

Figure 24 shows the thrust lines corresponding to two rows of anchors. In each line, two abrupt changes are observed.

8 | CONCLUSIONS

This study shows the global method is very well qualified for the stability analysis of anchored slopes, not only for the calculation of the safety factor of landslides but also for the location of the critical slip surface.

The stabilization effect of anchors lies mainly in the pre-tension that directly resists the slip body against sliding down, rather than increases the friction along the slip surface purely caused by the pre-tension.

The global method-based optimization model for locating the critical slip surface has weak nonlinearity compared with other existing optimization models, and easy to solve using those conventional optimization procedures.

The anchoring position is of vital importance to the stability of slopes, having an optimal value at which the anchored slope is stabilized best.

The best anchoring position might be outside the critical slip body.

ACKNOWLEDGEMENTS

This study is supported by the National Basic Research Program of China (973 Program), under the Grant No. 2014CB047100, and the National Natural Science Foundation of China, under the Grant Nos. 11172313 and 51538001.

ORCID

Hong Zheng http://orcid.org/0000-0002-8108-3009

REFERENCES

1. Abramson LW, Lee TS, Sharma S, et al. *Slope stability and stabilization methods*. New York: Springer; 1996.
2. Bromhead EN. *The Stability of Slopes*. London: Blackie Academic & Professional; 1992.
3. Cai F, Ugai K. Reinforcing mechanism of anchors in slopes: a numerical comparison of results of LEM and FEM. *Int J Numer Anal Methods Geomech*. 2003;27(7):549-564.
4. Zheng H, Liu DF, Li CG. Slope stability analysis based on elasto-plastic finite element method. *Int J Numer Methods Eng*. 2005;64(14):1871-1888.
5. Hryciw RD. Anchor design for slope stabilization by surface loading. *J Geotech Eng ASCE*. 1991;117(8):1260-1274.
6. Li L, Robert Y, Liu H. System reliability analysis for anchor-stabilised slopes considering stochastic corrosion of anchors. *Struct Infrastruct Eng*. 2015;11(10):1294-1305–56.
7. Zhu DY, Lee CF, Chan DH, Jiang HD. Evaluation of the stability of anchor-reinforced slopes. *Can Geotech J*. 2005;42(5):1342-1349.
8. Li X, He S, Wu Y. Limit analysis of the stability of slopes reinforced with anchors. *Int J Numer Anal Methods Geomech*. 2012;36(17):1898-1908.
9. Bishop AW. The use of the slip circle in the stability analysis of slopes. *Geotechnique*. 1955;5(1):7-17.
10. Bell JM. General slope stability analysis. *J Soil Mech Found Div Am Soc Civ Eng*. 1996;94(SM6):1253-1270.
11. Zhu DY, Lee CF. Explicit limit equilibrium solution for slope stability. *Int J Numer Anal Methods Geomech*. 2002;26(15):1573-1590.
12. Zheng H, Tham LG. Improved Bell's method for the stability analysis of slopes. *Int J Numer Anal Methods Geomech*. 2009;33(14):1673-1689.
13. Zheng H, Zhou CB. Global analysis on slope stability and its engineering application. *Sci China, Ser E*. 2009;52(2):507-512.
14. Zheng H. Eigenvalue problem from the stability analysis of slopes. *J Geotech Geoenviron Eng ASCE*. 2009;135(5):647-656.
15. Cheng YM, Li L, Chi SC. Performance studies on six heuristic global optimization methods in the location of critical slip surface. *Comput Geotech*. 2007;34(6):462-484.
16. Cheng YM, Li L, Lansivaara T, Chi SC, Sun YJ. An improved harmony search minimization algorithm using different slip surface generation methods for slope stability analysis. *Eng Optim*. 2008;40(2):95-115.
17. Baker R. Determination of the critical slip surface in slope stability computations. *Int J Numer Anal Methods Geomech*. 1980;4(4):333-359.
18. Yamagami T, Jiang JC. A search for the critical slip surface in three-dimensional slope stability analysis. *Soils Found*. 1997;37(3):1-6.
19. Chen Z, Shao C. Evaluation of minimum factor of safety in slope stability analysis. *Can Geotech J*. 1983;25(4):735-748.
20. Li YC, Chen Y M, Tony LT, et al. An efficient approach for locating the critical slip surface in slope stability analyses using a real-coded genetic algorithm. *Can Geotech J*. 2010;47(7):806-820.
21. Cheng YM, Li L, Chi SC, Wei WB. Determination of the critical slip surface using artificial fish swarms algorithm. *J Geotech Geoenviron Eng ASCE*. 2008;134(2):244-251.
22. Zhu DY. A method for locating critical slip surfaces in slope stability analysis. *Can Geotech J*. 2001;38(2):328-337.
23. Sun C, Li CG, Zheng H. Searching critical slip surfaces of slope based on global stability analysis (in Chinese). *Rock Soil Mech*. 2013;34(9):2583-2588.

How to cite this article: Zhang T, Zheng H, Sun C. Global method for stability analysis of anchored slopes. *Int J Numer Anal Methods Geomech*. 2018;1–14. https://doi.org/10.1002/nag.2856